Conversions of methane to synthesis gas over Co/γ-Al_2O_3 by CO_2 and/or O_2

H.Y. Wang and E. Ruckenstein *

Department of Chemical Engineering, State University of New York at Buffalo, Amherst, NY 14260, USA
E-mail: feaeliru@acsu.buffalo.edu

Received 21 February 2001; accepted 23 May 2001

The goal of the paper was to investigate the effect of the catalyst precursor on the catalytic activity. For this reason, the structure, the reducibility and the reaction behavior of γ-Al_2O_3-supported Co (24 wt%) catalysts as a function of calcination temperature (T_c) were investigated using X-ray diffraction, temperature-programmed reduction, CO chemisorption, pulse reaction with pure CH_4, and the catalytic reactions of methane conversion to synthesis gas. Depending on T_c, one, two, or three of the following Co-containing compounds, Co_3O_4, Co_2AlO_4, and $CoAl_2O_4$, were identified. Their reducibility decreased in the sequence: Co_3O_4 > Co_2AlO_4 > $CoAl_2O_4$. Co_3O_4 was generated as a major phase at a T_c of 500 °C and Co_2AlO_4 and $CoAl_2O_4$ at a T_c of 1000 °C. The reduced Co/γ-Al_2O_3 catalysts, obtained *via* the reduction of the 500 and 1000 °C calcined catalysts, provided high and stable activities for the partial oxidation of methane and the combined partial oxidation and CO_2 reforming of methane. They deactivated, however, rapidly in the CO_2 reforming of methane. Possible explanations for the stability are provided.

KEY WORDS: CO_2 reforming; partial oxidation; methane; synthesis gas; Co catalyst

1. Introduction

Owing to the increased demand for syngas (a mixture of H_2 and CO) for the syntheses of methanol and hydrocarbons, its preparation has received increased attention in recent years. Currently, the steam reforming of methane is the dominant commercial process. However, this process is highly endothermic and provides a synthesis gas with a too high H_2/CO ratio (>3) [1,2]. Recently, major efforts have been concentrated on the CO_2 reforming [3–12], the partial oxidation [13–24], and the combined partial oxidation and CO_2 reforming or H_2O reforming or both [25–27]. The CO_2 reforming provides a low H_2/CO ratio (around 1), which is suitable for the Fischer–Tropsch synthesis of higher hydrocarbons, and CO_2, a greenhouse gas, is thus consumed in a useful manner. The partial oxidation attracted attention due to its mild exothermicity and suitable H_2/CO ratio (around 2.0) obtained. The combined reactions also have a number of advantages. Firstly, by coupling the exothermic partial oxidation reaction with the endothermic reforming reaction, the methane-to-syngas conversion can be operated in a safer manner than the partial oxidation and in a more energy efficient manner than the reforming process. Secondly, by changing the feed composition, one can control the product ratio of H_2/CO and thus the selectivity to various Fischer–Tropsch synthesis products. Finally, one can conveniently use those natural gas reserves that contain substantial amounts of CO_2.

The conventional supported metal catalysts are usually prepared *via* the reduction of metal oxide precursors. In contrast, in a number of recent contributions, the metal was initially inserted in a well-defined structure, which was usually more difficult to reduce than the metal oxide. Ru-containing pyrochlores, such as Ln_2RuO_7 (Ln = Pr, Sm, Eu, Gd, *etc.*) [13], perovskites, such as $LaMO_3$ (M = Ni, Co, Rh) [17,20], spinels, such as $MgRh_2O_4$ [23], and solid solutions, such as NiO–MgO [7,11] and CoO–MgO [12,24] constitute such structures and have been used as precursors to obtain catalysts for the conversion of methane to syngas. In the present contribution, Co (Co_3O_4) and Co- and Al-containing compounds (Co_2AlO_4 and $CoAl_2O_4$) were prepared by changing the calcination temperature and used as precursors of metallic Co. The catalytic reactions investigated include: (i) CO_2 reforming of methane, (ii) partial oxidation of methane, and (iii) the combination of (i) and (ii).

2. Experimental

2.1. Catalyst preparation

The γ-Al_2O_3-supported catalysts were prepared by impregnating γ-Al_2O_3 with aqueous solutions of $Co(NO_3)_2 \cdot 6H_2O$, followed by overnight drying at 110 °C and calcination in the open air of a furnace for 8 h at various temperatures ranging from 500 to 1000 °C. The calcined catalysts will be denoted as Co(O)/γ-Al_2O_3(T_c), the temperature inside the parentheses indicating the calcination temperature. The catalysts reduced in H_2 will be denoted as Co/γ-Al_2O_3. Co loading means wt% Co in the completely reduced catalyst.

* To whom correspondence should be addressed.

1011-372X/01/0800-0013$19.50/0

2.2. Catalytic reaction

All the catalysts were tested under atmospheric pressure in a fixed-bed vertical quartz reactor (ID 4 mm) operated in a down flow mode with the catalyst held on a quartz wool bed. Before reaction, the catalysts were reduced *in situ* in a H_2 flow (30 ml/min) by increasing the temperature from room temperature to 600 °C at a rate of 20 °C/min and from 600 to 900 °C at a rate of 10 °C/min, without holding at 900 °C. After reduction, feed gases with a C/O atomic ratio of 1 were allowed to flow through the catalyst bed. The reactants and products were analyzed with an on-line gas chromatograph equipped with a Porapak Q column. An ice-cold trap was set between the reactor exit and the GC sampling valve to remove the water formed during reaction. The yields to H_2 and CO are defined as

$$\text{H}_2\text{ yield (\%)} = \frac{\text{H}_2}{2\text{CH}_{4,\text{in}}} \times 100,$$

$$\text{CO yield (\%)} = \frac{\text{CO}}{\text{CH}_{4,\text{in}} + \text{CO}_{2,\text{in}}} \times 100,$$

where H_2 and CO represent the moles of H_2 and CO produced per unit time, and $CH_{4,in}$ and $CO_{2,in}$ the moles introduced per unit time.

The blank tests, carried out with CO_2/CH_4 (1/1), CH_4/O_2 (2/1) and $CH_4/CO_2/O_2$ (4/2/1) in a reactor free of catalyst, indicated that the yields to CO and H_2 were negligible.

2.3. Catalyst characterization

The BET surface area of the calcined catalysts and the exposed Co surface area of the reduced catalysts were determined as in our previous paper [12]. The CH_4 decomposition, the temperature-programmed reduction (TPR), and the X-ray diffraction (XRD) were carried out as described previously [12].

3. Results

3.1. Catalytic reactions with mixtures of CH_4, CO_2 and O_2 of different compositions

The reduced Co/γ-Al_2O_3 catalysts, obtained *via* the reduction of Co(O)/γ-Al_2O_3(500 °C) or Co(O)/γ-Al_2O_3 (1000 °C), were used to catalyze the conversion of methane to synthesis gas. As shown in table 1, both Co/γ-Al_2O_3 catalysts provided initially high activities for the three reactions investigated, the synthesis gas yield being higher than 90%. The molar ratio of H_2/CO produced was about 1.1 in the CO_2 reforming, about 2.0 in the partial oxidation, and about 1.4 in the combined reaction.

The time-dependent activities of the Co/γ-Al_2O_3 catalysts are plotted in figures 1–3. In the CO_2 reforming of methane, both catalysts deactivated rapidly as indicated by the rapid decreases both in the conversions of CH_4 and CO_2 and in the flow rate of the exit gas with time on stream (figure 1 (a) and (b)). After 8 h of reaction, both catalysts were coated with notable amounts of coke, as indicated by their increased volumes. In the partial oxidation reaction, over both catalysts, no significant decreases in CH_4 conversion and CO (H_2 as well) selectivity were noted over 118 h on stream (figure 2). The two catalysts provided comparable activities during the entire period of study. In the combined partial oxidation and CO_2 reforming of methane, after an activation period, the CH_4 (CO_2 as well) conversion and CO (H_2 as well) yield remained high and unchanged during the period of study of 125 h over both catalysts (figure 3). The effect of O_2/CO_2 ratio (while maintaining a total flow rate of 35 ml/min and a C/O atomic ratio of 1) on the CO yield and H_2/CO ratio in the combined reaction was investigated over the Co/γ-Al_2O_3(1000 °C). The results are presented in figure 4. The CO yield remained almost the same, while the H_2/CO ratio increased from 1.40 to 1.85 with increasing O_2/CO_2 ratio from 0.5 to 4.0. The combined reaction can provide a H_2/CO ratio between 1 and 2, the stoichiometric values corresponding to the CO_2 reforming of methane and partial oxidation of methane, respectively. While in the partial oxidation of methane, bright hot spots were always observed on the surface of the catalyst [28,29] (they were

Table 1
Effect of calcination temperature (T_c) on the initial activity of the 24 wt% Co/γ-Al_2O_3 in catalytic reactions of mixtures of CH_4, CO_2, and O_2.[a]

Feed composition (%)			T_r[b]	SV[c]	T_c	CH_4 conversion	H_2 yield	CO yield	H_2/CO
CH_4	CO_2	O_2	(°C)	(ml/g h)	(°C)	(%)	(%)	(%)	ratio
50.0	50.0	0.0	900	60 000	500	95.6	96.0	96.4	1.14
					1000	95.0	95.4	96.2	1.15
57.1	28.6	14.3	900	105 000	500	92.8	92.0	92.1	1.42
					1000	91.0	89.6	90.6	1.36
66.6	0.0	33.4	850	360 000	500	95.0	93.6	92.9	2.02
					1000	95.0	92.3	92.8	1.99

[a] Data obtained after 10 min on stream.
[b] Reaction temperature.
[c] Space velocity.

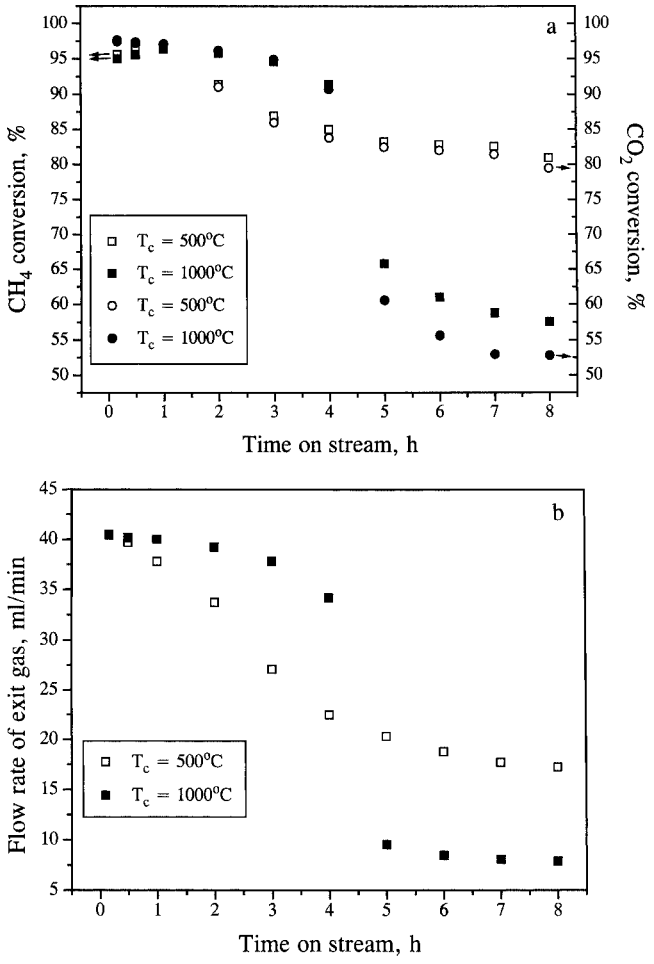

Figure 1. Time-dependent conversions of CH_4 and CO_2 (a) and the flow rate of exit gas (b) as a function of time on stream in CO_2 reforming of methane over the 24 wt% Co/γ-Al_2O_3(T_c) catalysts. P = 1 atm, T = 900 °C, amount of catalyst = 20.0 mg, CH_4/CO_2 = 1/1, space velocity = 60 000 ml/h g.

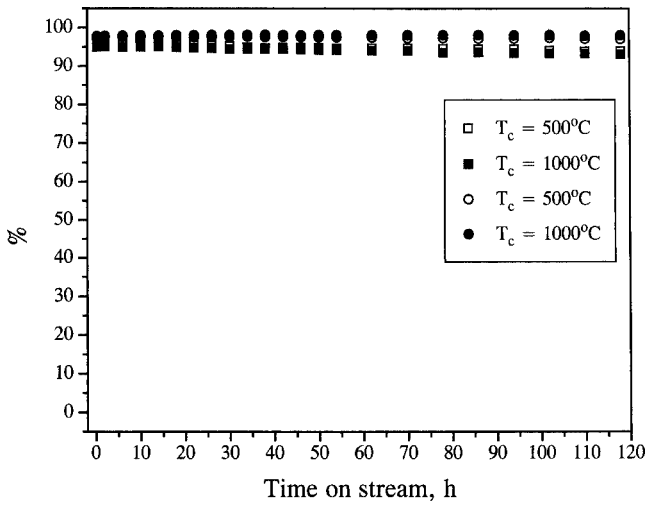

Figure 2. Time-dependent CH_4 conversion (□, ■) and CO selectivity (○, ●) in partial oxidation of methane over the 24 wt% Co/γ-Al_2O_3(T_c) catalysts. P = 1 atm, T = 850 °C, amount of catalyst = 10.0 mg, CH_4/O_2 = 2/1, space velocity = 360 000 ml/h g.

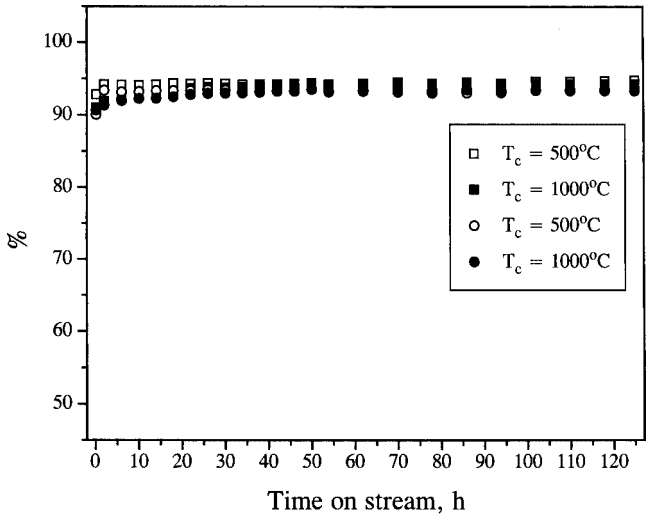

Figure 3. Time-dependent CH_4 conversion (□, ■) and CO yield (○, ●) in combined partial oxidation and CO_2 reforming of methane over the 24 wt% Co/γ-Al_2O_3(T_c) catalysts. P = 1 atm, T = 900 °C, amount of catalyst = 20.0 mg, $CH_4/CO_2/O_2$ = 4/2/1, space velocity = 105 000 ml/h g.

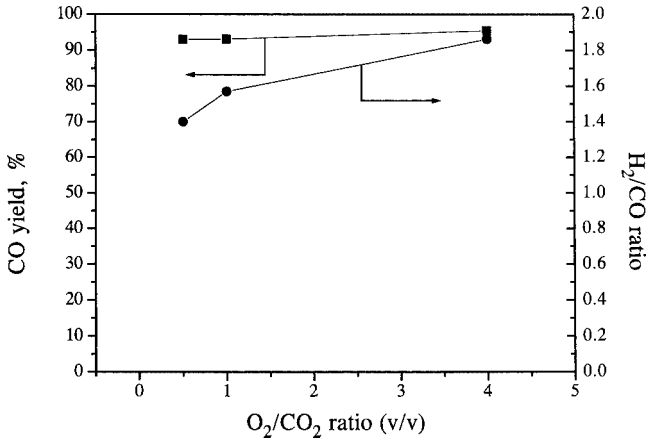

Figure 4. CO yield and H_2/CO ratio as a function of O_2/CO_2 in combined reaction over the 24 wt% Co/γ-Al_2O_3(1000 °C) (data obtained after 30 h of reaction). P = 1 atm, T = 900 °C, amount of catalyst = 20.0 mg, $CH_4/(CO_2 + 2O_2)$ = 1/1, space velocity = 105 000 ml/h g.

visually observed in the present work as well), in the combined reaction less bright hot spots could be noted visually for the molar feed ratios $CH_4/CO_2/O_2$ = 3/1/1 and 9/1/4 but not for 4/2/1.

3.2. Physico-chemical characterization

3.2.1. BET surface area of the calcined catalysts and exposed metallic Co surface area of the reduced catalysts

The BET surface area and the exposed Co surface area were determined before and after reduction, respectively. As shown in table 2, both the BET surface area and the exposed metal surface area were much higher for T_c = 500 °C than for T_c = 1000 °C.

Table 2
Physical data for the γ-Al_2O_3-supported Co (24 wt%) catalysts.

T_c (°C)	BET surf. area[a] (m^2/g)	Co surf. area[b] (m^2/g-cat.) $\times 100$
500	51	213
1000	23	65

[a] For the calcined catalysts.
[b] For the reduced catalysts.

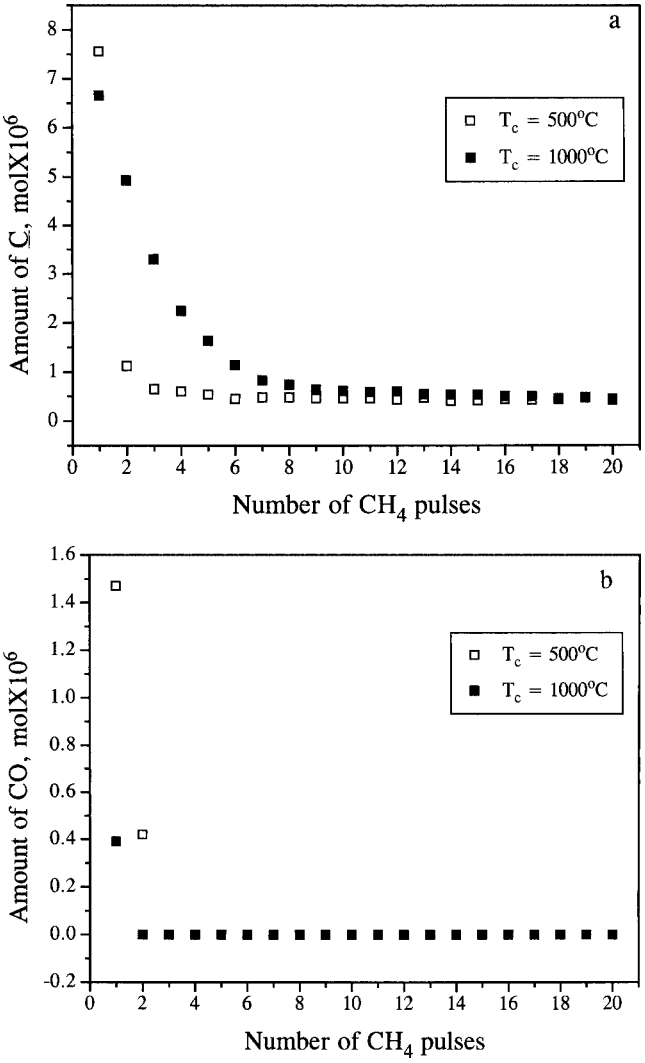

Figure 5. Amount of carbon (C) (a) and CO (b) formed during CH_4 decomposition as a function of number of CH_4 pulses over the 24 wt% Co/γ-Al_2O_3(T_c) catalysts at 900 °C.

3.2.2. Surface carbon formed during the CH_4 decomposition

The decomposition of CH_4 pulses over the reduced catalysts was carried out at 900 °C and the amount of surface carbon (C) generated was determined from the carbon balance. Figure 5 plots the amounts of C and CO formed during each pulse as a function of the number of CH_4 pulses. The amount of C generated during the first pulse was somewhat higher for $T_c = 500$ °C than for $T_c = 1000$ °C; it was, however, much lower for the former in the following five pulses (figure 5(a)). CO was detected during the first one or two pulses and its amount was about four times larger for $T_c = 1000$ °C (figure 5(b)). As shown in table 3, with the exception of the first pulse, the accumulated amount of C during the same period was higher for $T_c = 1000$ °C than for $T_c = 500$ °C.

3.2.3. Compounds present in the calcined catalysts

The species present in the calcined catalysts were identified by XRD and TPR. Figure 6 presents the XRD patterns for the 800 °C calcined catalyst. Some of the peaks can be attributed to Al_2O_3, while all the other peaks to any of the compounds Co_3O_4, Co_2AlO_4, and $CoAl_2O_4$. It is, therefore, difficult to identify by XRD the Co-containing phases. The above three compounds have a spinel structure with the interactions increasing in strength as the mumber of Al^{3+} ions in the surrounding of the Co ion increases [30]. Consequently, the reducibility should decrease in the sequence: $Co_3O_4 > Co_2AlO_4 > CoAl_2O_4$. TPR experiments were carried out to help to identify the species present. Fig-

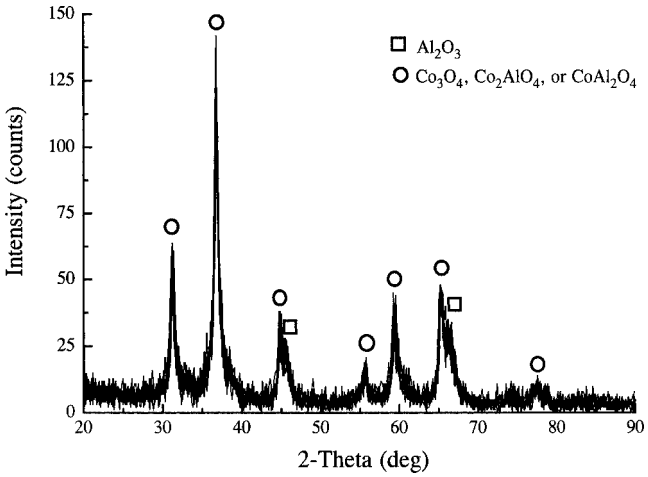

Figure 6. XRD pattern of the 24 wt% Co(O)/γ-Al_2O_3(800 °C).

Table 3
Amount of carbon deposited during CH_4 decomposition over the reduced supported Co (24 wt% loading) catalysts at 900 °C.

Catalyst	C formed during various numbers of CH_4 pulses (μmol)				
	1st pulse	1st 3 pulses	1st 5 pulses	1st 10 pulses	1st 20 pulses
Co/γ-Al_2O_3(500 °C)	7.6	9.3	10.5	12.8	17.2
Co/γ-Al_2O_3(1000 °C)	6.7	14.9	18.8	22.7	27.9
Co/MgO(800 °C)	1.7	4.1	5.3	7.7	11.9

ure 7 provides the TPR patterns of the catalysts calcined at various temperatures as well as those of the mixture of $Co_3O_4/CoAl_2O_4$, and table 4 lists the peak temperatures T_m. For the mixture of $Co_3O_4/CoAl_2O_4$, two peaks were observed: one at about 340 °C, which can be attributed to the reduction of Co_3O_4, and the other at about 940 °C, which is due to the reduction of $CoAl_2O_4$. The TPR peaks observed over the calcined Co(O)/γ-Al_2O_3 catalysts can be divided into three regions: region I (<500 °C), region II (500–900 °C), and region III (>900 °C). For the Co(O)/γ-Al_2O_3(500 °C), only a peak in region I was noted. For the Co(O)/γ-Al_2O_3(700 °C), two peaks, one in region I and another in region II, were identified. For the Co(O)/γ-Al_2O_3(800 °C) and Co(O)/γ-Al_2O_3(900 °C), three peaks, one in each of the regions, were noted. Finally, for the Co(O)/γ-Al_2O_3(1000 °C), two peaks, one in region II and the other in region III, were observed. According to the reducibility sequence of the three compounds, the TPR peak in region I can be attributed to Co_3O_4, that in region II to Co_2AlO_4, and that in region III to $CoAl_2O_4$. Consequently, Co_3O_4 was identified as the major phase in the 500 °C calcined catalyst, Co_3O_4 and Co_2AlO_4 in the 700 °C, Co_3O_4, Co_2AlO_4 and $CoAl_2O_4$ in the 800 and 900 °C, and Co_2AlO_4 and $CoAl_2O_4$ in the 1000 °C calcined catalysts. With increasing calcination temperature, a positive shift in the TPR peak in each of the regions was noted, indicating an increasing strength of the interaction between the species and support.

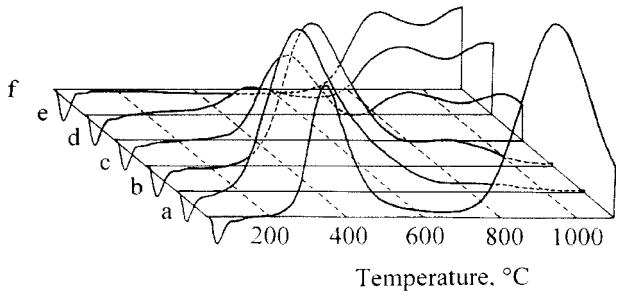

Figure 7. TPR profiles of the mixture of $Co_3O_4/CoAl_2O_4$ (a) and the 24 wt% Co(O)/γ-Al_2O_3 catalysts calcined at 500 (b), 700 (c), 800 (d), 900 (e), and 1000 °C (f).

Table 4
Temperature-programmed reduction of the mixture of $Co_3O_4/CoAl_2O_4$ and of the calcined 24 wt% Co(O)/Al_2O_3 catalysts.

Sample	T_c[a] (°C)	T_m[b] (°C)		
		Region I	Region II	Region III
$Co_3O_4/CoAl_2O_4$	–	340	–	940
Co(O)/Al_2O_3	500	350	–	–
	700	460	830	–
	800	485	810	1045
	900	480	860	>1000
	1000	–	880	>1000

[a] Calcination temperature.
[b] T_m = peak temperature; region I (<500 °C), region II (500–900 °C), and region III (>900 °C).

4. Discussion

4.1. Effect of calcination temperature on the species formed and the reducibility of the calcined catalysts

The impregnation of γ-Al_2O_3 with an aqueous cobalt nitrate solution followed by drying at 110 °C led initially to the formation of Co_3O_4 on the surface of the support [31–33]. Co_3O_4 has the composition $Co^{2+}(Co_2^{3+})O_4$, with Co^{2+} ions located in the tetrahedrally coordinated sites and Co^{3+} ions in the octahedrally coordinated sites. The calcination led to the decomposition of Co_3O_4 and the ion exchange between Co_3O_4 and Al_2O_3. While the tetrahedral sites remained occupied by Co^{2+}, the Co^{3+} were substituted by Al^{3+}, thus leading to the formation of Co_2AlO_4 and $CoAl_2O_4$. The incorporation of Co^{2+} into the tetrahedral sites of the support can also generate $CoAl_2O_4$. These structures were formed because γ-Al_2O_3 has the structure of a spinel with a deficit of cations [34]. A simultaneous decrease of the intensity of the peak in region I and increase of those in regions II and III could be observed with increasing T_c from 500 to 1000 °C (figure 7), indicating that Co_3O_4 was converted to the other two phases. Co_3O_4 remained as the major phase at $T_c = 500$ °C, while the entire Co_3O_4 was converted to Co_2AlO_4 and $CoAl_2O_4$ at $T_c = 1000$ °C.

The exposed metal surface area of the Co/γ-Al_2O_3 (1000 °C) was much lower than that of the Co/γ-Al_2O_3 (500 °C) (table 2) because the species formed in the former case during calcination (Co_2AlO_4 and $CoAl_2O_4$) are less reducible than that formed in the latter (Co_3O_4).

4.2. Catalytic conversion of methane to synthesis gas

4.2.1. Effect of O_2 addition

Both Co/γ-Al_2O_3(500 °C) and Co/γ-Al_2O_3(1000 °C) provided high and stable activities for the partial oxidation of methane and for the combined partial oxidation and CO_2 reforming of methane, but an unstable activity for the CO_2 reforming of methane (figures 1–3). The carbon deposition and the metal sintering are the main causes for catalyst deactivation in the methane conversion reactions, which are usually carried out at high temperatures (>800 °C). Sintering decreases not only the number of active sites, but also stimulates the carbon deposition, because large metal ensembles favor coke formation [35]. When O_2 was present in the feed, less carbon was formed on the catalyst than during the CO_2 reforming. This is similar to the observation that an excess of CO_2 in the feed stream suppressed carbon formation in the CO_2 reforming of methane [5,36]. Moreover, in all three methane conversion reactions, the atmosphere in the reactor was both reductive and oxidative, due to the coexistence of reductive (CH_4, H_2 and CO) and oxidative (CO_2 and/or O_2, and H_2O) species. While the reductive atmosphere stimulated metal sintering, the oxidative atmosphere favored its redispersion [37]. These two opposite effects may cancel out each other. A steady state can be achieved more easily in the partial oxidation and the combined reaction than in the CO_2 reforming due to the presence of O_2 in the former two reactions. For these reasons, the Co/γ-Al_2O_3 catalysts exhibited

high and stable activities for the partial oxidation of methane and the combined reaction.

4.2.2. Effect of calcination temperature (T_c)

The starting idea of the present paper was to generate different species by varying the calcination temperature in order to control the reducibility of catalyst and its catalytic performance. The higher the reducibility, the larger the size of metal particles was expected to be. Since large metal ensembles stimulate coke formation, Co/γ-Al_2O_3(1000 °C) was expected to generate less carbon in the decomposition of pure CH_4 than Co/γ-Al_2O_3(500 °C). However, as shown in table 3, with the exception of the first pulse, the accumulated amount of $\underline{C}$ during the same period was higher for $T_c = 1000$ °C than for $T_c = 500$ °C. The higher accumulation of $\underline{C}$ during the first pulse for $T_c = 500$ °C was caused by the larger number of metallic sites present. The change in behavior for the latter several pulses was due to the generation of new accessible metallic sites *via* the reduction of Co_2AlO_4 and $CoAl_2O_4$ by CH_4 (as indicated by the formation of a notable amount of CO (figure 5(b))) in the 1000 °C calcined catalyst. As shown in table 3, compared to the 24 wt% Co/MgO(800 °C), which provided a high and stable activity for the CO_2 reforming of methane [38], both the 24 wt% Co/γ-Al_2O_3(500 °C) and the 24 wt% Co/γ-Al_2O_3(1000 °C) exhibited much higher carbon depositions. For this reason, severe deactivation occurred over both catalysts (figure 1).

For the partial oxidation of methane, both Co/γ-Al_2O_3 (500 °C) and Co/γ-Al_2O_3(1000 °C) provided comparable activities with time on stream (figure 2). The almost equal methane conversions occurred most likely because under the conditions employed the number of metallic sites was sufficiently large for thermodynamic equilibrium to be achieved in both cases [24].

In the combined partial oxidation and CO_2 reforming of methane, Co/γ-Al_2O_3(1000 °C) provided a somewhat lower initial activity than Co/γ-Al_2O_3(500 °C) (figure 3). This reflected the trend of the exposed Co surface area (table 2), revealing that the metallic sites were the active sites for the synthesis gas formation. The activation period observed over Co/γ-Al_2O_3(1000 °C) indicated that additional metallic sites were generated during reaction *via* the reduction of Co_2AlO_4 and $CoAl_2O_4$ by CH_4 and/or H_2. Both catalysts exhibited comparable activities after 30 h on stream; this occurred most likely because thermodynamic equilibrium was achieved in both cases. Compared to the partial oxidation, less bright or no hot spots were visually observed. Consequently, the combined reaction can be operated in a safer manner than the partial oxidation.

5. Conclusions

The structural characteristics of the γ-Al_2O_3-supported Co (24 wt%) catalysts were strongly affected by the calcination temperature (T_c), and so was their reducibility. Co_3O_4 was generated as a major phase at a T_c of 500 °C and Co_2AlO_4 and $CoAl_2O_4$ at a T_c of 1000 °C. The reducibility of the γ-Al_2O_3-supported Co catalysts decreased with increasing T_c because of the formation of the less reducible Co_2AlO_4 and $CoAl_2O_4$. No significant effect of T_c on the catalytic performance was, however, observed. Both the 24 wt% Co/γ-Al_2O_3(500 °C) and the 24 wt% Co/γ-Al_2O_3(1000 °C) provided high and stable activities for the partial oxidation of methane and the combined partial oxidation and CO_2 reforming of methane, but an unstable activity for the CO_2 reforming of methane.

References

[1] J.R. Rostrup-Nielsen, Catal. Today 18 (1993) 305.
[2] J.M. Fox, III, Catal. Rev. Sci. Eng. 35 (1993) 169.
[3] A.M. Gadalla and B. Bower, Chem. Eng. Sci. 43 (1988) 3049.
[4] J.T. Richardson and S.A. Paripatyadar, Appl. Catal. 61 (1990) 293.
[5] A.T. Ashcroft, A.K. Cheetham, M.L.H. Green and P.D.F. Vernon, Nature 352 (1991) 225.
[6] J.R. Rostrup-Nielsen and J.-H.B. Hansen, J. Catal. 144 (1993) 38.
[7] E. Ruckenstein and Y.H. Hu, Appl. Catal. A 133 (1995) 149.
[8] V.C.H. Kroll, H.M. Swaan and C. Mirodatos, J. Catal. 161 (1996) 409.
[9] R.N. Bhat and W.M.H. Sachtler, Appl. Catal. A 150 (1997) 279.
[10] S.M. Stagg, E. Romeo, C. Padro and D.E. Resasco, J. Catal. 178 (1998) 137.
[11] K. Tomishige, Y. Chen and K. Fujimoto, J. Catal. 181 (1999) 91.
[12] E. Ruckenstein and H.Y. Wang, Appl. Catal. A 204 (2000) 257.
[13] A.T. Ashcroft, A.K. Cheetham, J.S. Foord *et al.*, Nature 344 (1990) 319.
[14] D. Dissanayake, M.P. Rosynek, K.C.C. Kharas and L.H. Lunsford, J. Catal. 132 (1991) 117.
[15] D.A. Hickman and L.D. Schmidt, J. Catal. 138 (1992) 267.
[16] D.A. Hickman and L.D. Schmidt, Science 259 (1993) 343.
[17] A. Slagtern and U. Olsbye, Appl. Catal. A 110 (1994) 99.
[18] V.R. Choudhary, B.S. Uphade and A.S. Mamman, Catal. Lett. 32 (1995) 387.
[19] A. Santos, M. Menéndez, A. Monzón *et al.*, J. Catal. 158 (1996) 83.
[20] R. Lago, G. Bini, M.A. Pena and J.L.G. Fierro, J. Catal. 167 (1997) 198.
[21] V.A. Tsipouriari, Z. Zhang and X.E.J. Verykios, J. Catal. 179 (1998) 283.
[22] E. Ruckenstein and Y.H. Hu, Appl. Catal. A 183 (1999) 85.
[23] H.Y. Wang and E. Ruckenstein, J. Catal. 186 (1999) 181.
[24] H.Y. Wang and E. Ruckenstein, J. Catal. 199 (2001) 309.
[25] V.R. Choudhary, B.S. Uphade and A.A. Belhekar, J. Catal. 163 (1996) 312.
[26] A.M. O'Connor and J.R.H. Ross, Catal. Today 46 (1998) 203.
[27] E. Ruckenstein and Y.H. Hu, Ind. Eng. Chem. Res. 37 (1998) 1744.
[28] D. Dissanayake, M.P. Rosynek and J.H. Lunsford, J. Phys. Chem. 97 (1993) 3644.
[29] Y.F. Chang and H. Heinemann, Catal. Lett. 21 (1993) 215.
[30] P. Arnoldy and J.A. Moulijn, J. Catal. 93 (1985) 38.
[31] K.S. Chung and F.E. Massoth, J. Catal. 64 (1980) 320.
[32] M. LoJacono, J.L. Verbeck and G.C.A. Schuitt, J. Catal. 29 (1973) 463.
[33] R.L. Chin and D.M. Hercules, J. Phys. Chem. 86 (1982) 360.
[34] J.T. Richardson and L.W. Vernon, J. Phys. Chem. 62 (1958) 1153.
[35] J.R. Rostrup-Nielsen, in: *Catalysis Science and Technology*, Vol. 5 eds. J.R. Anderson and M. Boudart (Springer, Berlin, 1984) pp. 1–118.
[36] S. Teuner, Hydrocarbon Process. 64 (1985) 106.
[37] E. Ruckenstein, in: *Metal–Support Interactions in Catalysis, Sintering, and Redispersion*, eds. S.A. Stevenson, J.A. Dumesic, R.T.K. Baker and E. Ruckenstein (Van Nostrand Reinhold, New York, 1987) p. 297.
[38] H.Y. Wang and E. Ruckenstein, Appl. Catal. A 209 (2001) 207.